UDC669.14.018.2-462:629.11.011.66

High-Strength Steel Tubes for Automobile Door Impact Beams

Hiroto Tanabe*1 Akihiro Miyasaka*1
Kazumasa Yamazaki*1 Toshio Iwasaki*2
Hideo Akada*2

Abstract:

The bending deformation behavior of steel tubes for door impact beams used as reinforcement members against the side collision of passenger cars was experimentally studied. The deformation process may be divided into three steps: cross-sectional flattening, plastic collapse, and circumferential buckling. These deformation steps were examined together with the crush distance-applied load curves and absorbed energy characteristics, and the maximum load was estimated. The ductility required of door impact beams was determined from the deformation behavior, and a new electric resistance welded (ERW) steel tube with a tensile strength of 1,470 N/mm² class was developed to meet the ductility requirement.

1. Introduction

Automobile manufactures strengthen the doors of passenger cars using impact beams (reinforcement members) to reduce deaths and injuries in side collisions. The door impact beams are to absorb the kinetic energy of side collision through the initial deformation of the door, thereby reducing damage to the occupants in the passenger compartment. The door impact beams were traditionally made chiefly by press forming high-strength steel sheet. Today, steel tubes are increasing in this application because weight savings can be achieved through their use[1,2].

This report explains the deformation behavior of door impact beams that are made of steel tubes, lightweight, and capable of absorbing high energy. Also introduced here is the new high-strength electric resistance welded (ERW) steel tube developed specifically for application to door impact beams.

2. Bending Deformation Behavior of Steel Tubes for Door Impact Beams

A three-point bending test method was developed in accordance with the automobile side strength tests specified in JASO B 103-86 and FMVSS No. 214, in order to observe the plastic deformation behavior of steel tubes in the doors of passenger cars. The test method is schematically shown in **Fig. 1**. **Table 1** lists the chemical compositions and tensile strength of the steel tubes tested.

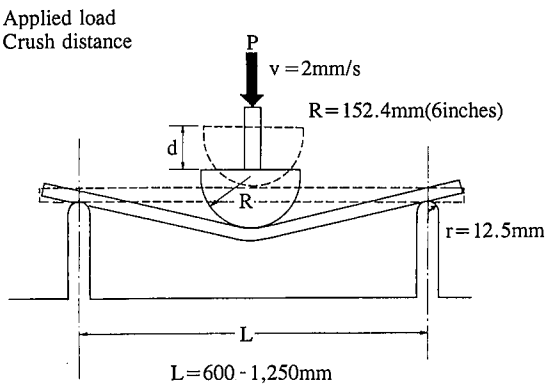

Fig. 1 Three-point bending test method

*1 Technical Development Bureau
*2 Nagoya Works

Table 1 Sizes and chemical compositions (mass%) of steel tubes

Diameter	Thickness	t/D×100	C	Si	Mn	Nb	Cr	Mo	B	TS
25.4-40.0mm	1.6-5.0mm	5-15%	0.14 - 0.30	0.15 - 0.23	0.80 - 1.60	- 0.03	- 0.30	- 0.40	- 0.002	583-1,840N/mm²

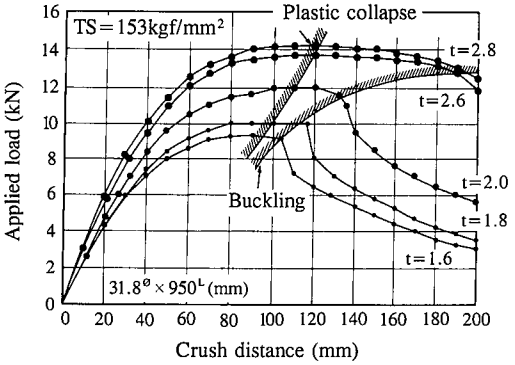

Fig. 2 Applied load-crush distance curves

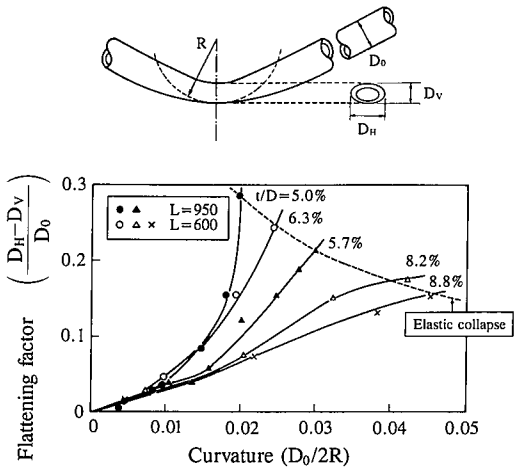

Fig. 3 Relationship between progress of bending and flattening

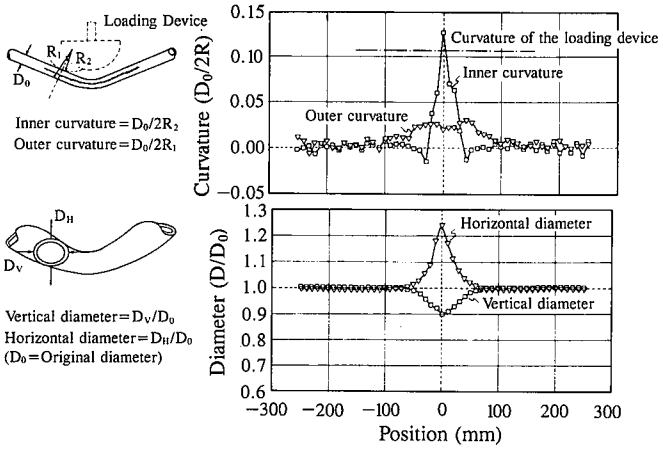

Fig. 4 Cross-sectional shape of tube right below loading device immediately after plastic collapse (31.8 mm ϕ × 1.8 mm t)

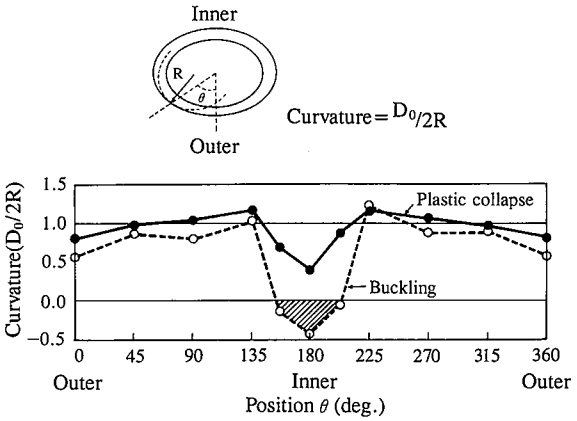

Fig. 5 Comparison of cross-sectional shape of tube immediately after plastic collapse and circumferential buckling (31.8 mm ϕ × 1.8 mm t)

Fig. 2 shows typical applied load-crush distance curves obtained in the three-point bending test. Corresponding to the stiffness of tubes, the applied load increases linearly with increasing crush distance, declines in the rate of increase, reaches the peak point, decreases slowly, and suddenly drops. **Fig. 3** shows the flattening of steel tubes just below the loading device. This flattening is the sum of flattening for reduction in the deformation energy of the bend derived from total strain theory[3] and flattening due to the concentrated load of the loading device[1,2]. The degree of flattening increases with decreasing wall thickness (t/D ratio) and decreasing span (increasing applied load). The progress of flattening influences the curvature of the bend at the onset of plastic collapse. **Fig. 4** shows the shape of a tube that has plastically collapsed[4,5]. The flattening of the tube is concentrated right below the loading device. The tube is longitudinally buckled so that the inner curvature of the bend is greater than the curvature of the loading device. The bending load in this case is equivalent to the maximum load shown in **Fig. 2**. Further travel of the loading device further the local flattening of the tube and increases the nonuniformity of the inner curvature. The decrease of load is moderate in this case, but sharply drops when the tube is circumferentially buckled as shown in **Fig. 5**. **Fig. 5** shows the distribution of circumferential curvature right below the loading device immediately after the plastic collapse and circumferential buckling. After the plastic collapse, the tube is progressively flattened, but has a convex (or plus) curvature around the circumference. After the circumferential buckling, the tube has a concave (or minus) curvature. The collapse of the inner surface of the bend is considered to cause a steep drop in the applied load. The bending deformation process of the tube runs through three steps: cross-sectional flattening, plastic collapse, and circumferential buckling.

Endo and Murota[5] proposed a method for estimating the

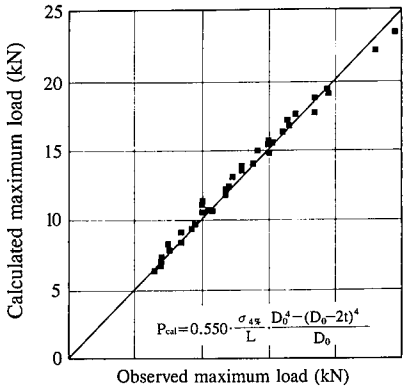

Fig. 6 Relationship between calculated and observed values of maximum bending load

maximum load, which is equivalent to the plastic collapse, from the bending moment taking into consideration the flattening of the tube. Their method succeeded in qualitatively determining the maximum load point, but not quantitatively[2], because the cross section of the tube is not of simple ovality right below the loading device. The following equation was derived to estimate the maximum load from experimental results[1,2]:

$$P_{cal} = 0.550\times(\sigma_{4\%}/L)\times((D_0^4-(D_0-2t)^4)/D_0) \quad (1)$$

where D_0 is the initial outside diameter of the tube before the bending test, t is the wall thickness of the tube, and L is the bending span. From the test results of various types of tubes, the flow stress at the 4% strain ($\sigma_{4\%}$) is used as material strength. The values of the maximum load calculated by Eq. (1) are compared with experimentally obtained values in **Fig. 6**. The calculated values agree well with the experimental values. This means that **Fig. 6** can be used to estimate the maximum load with high accuracy.

3. Ductility Required of Door Impact Beams

When the tube installed as an impact beam in a passenger car door is bent, it is subjected to large tensile deformation in the outer surface. When a crack is produced in the outer surface of the bend in the tube, it is likely not only to sharply reduce the bending load and absorbed energy, but also to intrude into the passenger compartment. The strain in the outer surface of the bend in the plastic collapse phenomenon was estimated and used to determine the ductility required of the tube as the door impact beam. **Fig. 7** shows the elongation presumed to occur on the outer side of the bend in the tube on the assumption that the tube is not flattened. As flattening actually takes place, however, an appropriate correction must be made to the data. **Fig. 8** shows the correction factor (indicated by solid circles) calculated from the measured strain on the outer side of the bend. This correction factor is considered to include the strain correction (indicated by open circles) due to the flattening of the tube and the strain correction (difference between the values indicated by the open and solid circles) due to the fact that the strain is rendered difficult to accumulate by the onset of plastic collapse in the early stage of the bending deformation process. These contributions are each expressed as a function of the wall thickness-to-outside diameter (t/D) ratio of the tube[2-5]. **Fig. 9** shows the relationship between the size and necessary elongation of door impact beam tubes.

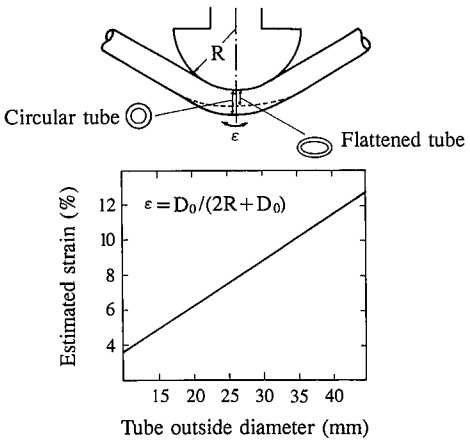

Fig. 7. Estimation of strain on outer side of bend when tube is not flattened

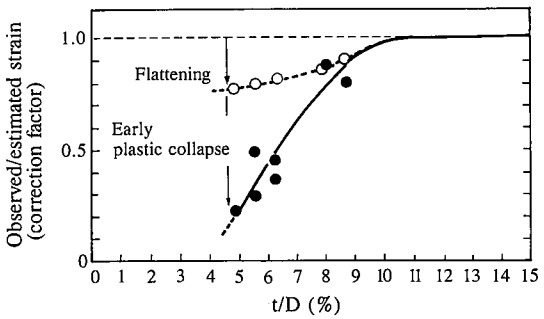

Fig. 8 Correction factor for strain on outer side of bend

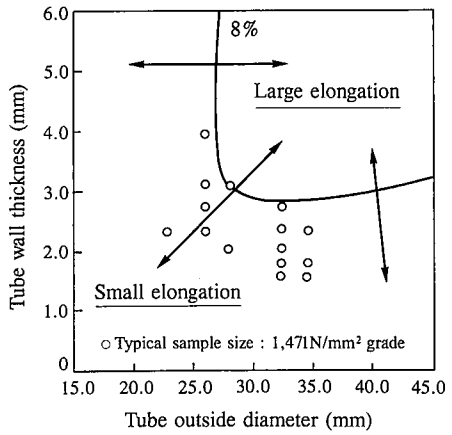

Fig. 9 Schematic diagram of ductility required on outer side of bend before plastic collapse

The outside diameter of the tube depends on the space available in the door, and its wall thickness on the necessary bending load and absorbed energy. Open circles in **Fig. 9** indicate the dimensions of typical high-strength steel tubes having a tensile strength of more than 1,470 N/mm² used as door impact beams. The figure shows that an elongation of more than 8% is required of door impact beam tubes of present dimensions that are subjected to bending deformation.

4. High-Strength Steel Tubes for Door Impact Beams

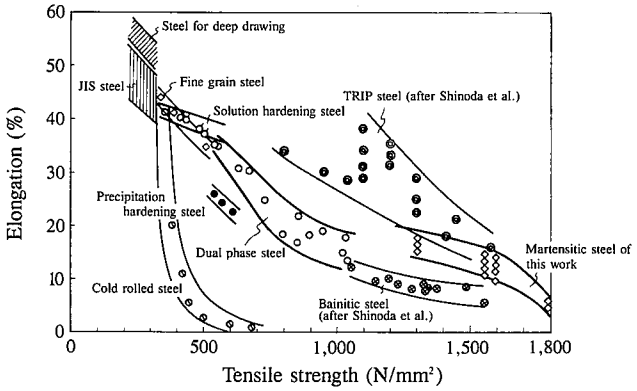

Fig. 10 Relationship between tensile strength and elongation of various steels[9,10]

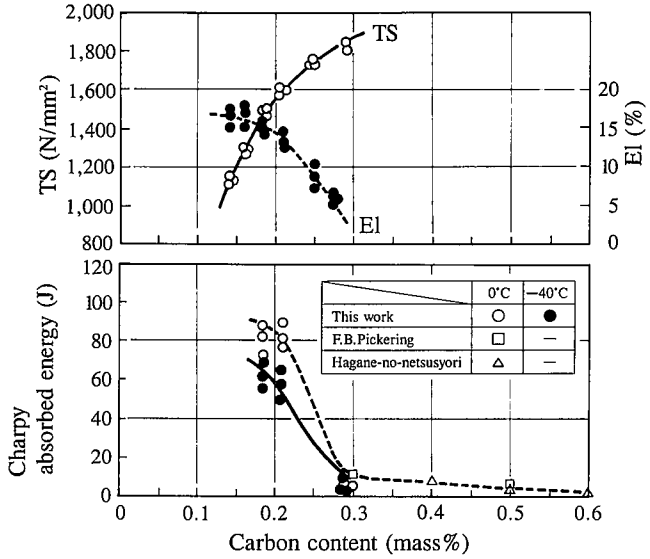

Fig. 11 Mechanical properties of martensitic steel[6]

As is clear from Equation (1), strengthening is effective in obtaining high bending strength with small weight. **Fig. 10** shows the relationship between strength and ductility in various types of high-strength steels[6,7]. Martensitic steels can be commercially produced by a low-cost process for application in door impact beams that must have an elongation of 8% or higher and tensile strength of 1,470 N/mm² or higher. The hardness of martensitic steel is derived mainly from carbon, with only small contributions from other elements[8-10]. **Fig. 11** shows the mechanical properties of steels with a carbon content of 0.15 to 0.30 mass% as quenched to obtain a martensite microstructure of more than 99%[2,9,10]. When the carbon content is 0.16 to 0.24 mass%, high strength, ductility, and toughness are accomplished despite a martensite microstructure in the as-quenched condition. A low-carbon (about 0.20 mass%C) martensite microstructure is effective in producing lightweight door impact beam tubes.

4.1 High-strength steel tube production process

Door impact beam tubes of low-carbon martensite microstructure are produced in the following way. Steel is adjusted as to the necessary carbon content, inclusion control and critical cooling rate, and is controlled rolled into strip of relatively low strength to reduce the load on the subsequent slitting and electric resistance welding processes. The strip can thus be efficiently slit and electric resistance welded into door impact beam tubing. The tubing is then induction hardened by the method illustrated in **Fig. 12** to provide the required strength and ductility. **Photo 1** shows the cross-sectional structures of the electric resistance weld metal and base metal. Induction hardening produces a uniform martensite microstructure including the weld metal with little surface decarburization. **Fig. 13** shows the tensile test results of a representative tube size. The tensile strength is higher than 1,470 N/mm², and the ductility is stably high (total elongation of more than 8%).

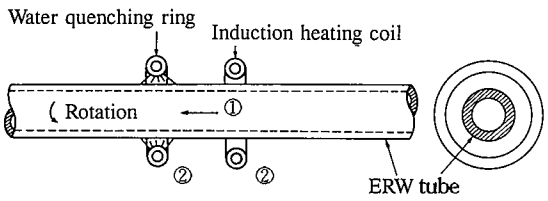

Fig. 12 Induction heating method

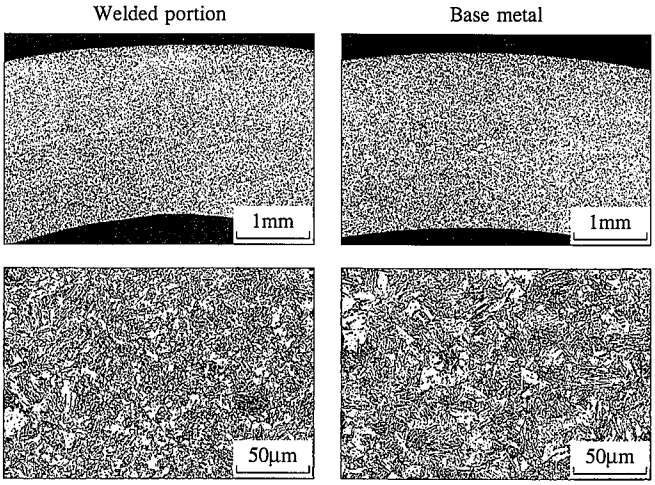

Photo 1 Cross-sectional structures of high-strength steel tube (STQM18RB, 25.4mm ϕ × 2.3 mm t)

4.2 Delayed fracture resistance

Door impact beam tubes with a tensile strength of 1,470 N/mm² or higher in the as-quenched condition are installed in the doors of passenger cars. Delayed fracture is generally feared in these high-strength steel tubes. The new ERW tube steel discussed here is increased in delayed fracture resistance by decreasing the amount of impurities, developing a fine-grained austenite microstructure, and reducing the residual stress. **Fig. 14** schematically shows the method of evaluating delayed fracture resistance. A notched tensile specimen was corroded in a 5%HCl solution and tested under a constant load. The test results are shown in **Fig. 15**. Delayed fracture was observed in none of the specimens that underwent tensile stress to notch fracture stress. The new ERW tube steel is low in delayed fracture sensitivity even in such an environment as shown in **Fig. 14**. Since the door impact beam is not always subjected to stress as under the delayed fracture test conditions, as-quenched ERW tubes can suffice as door reinforcement members.

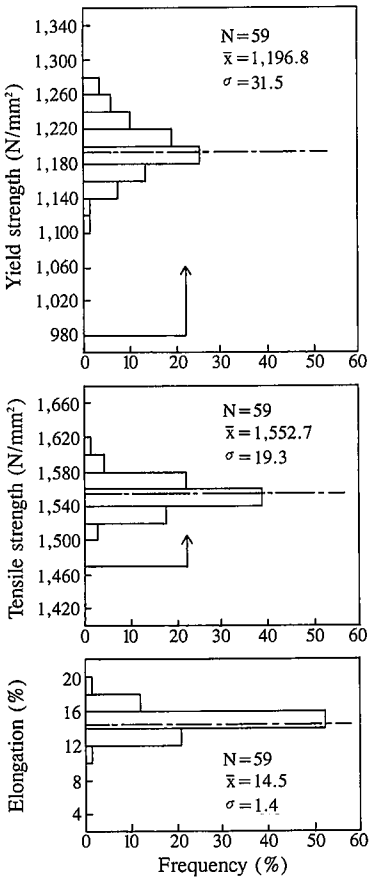

Fig. 13 Tensile test results (STQM18RB, 31.8 mm ϕ × 2.0 mm t)

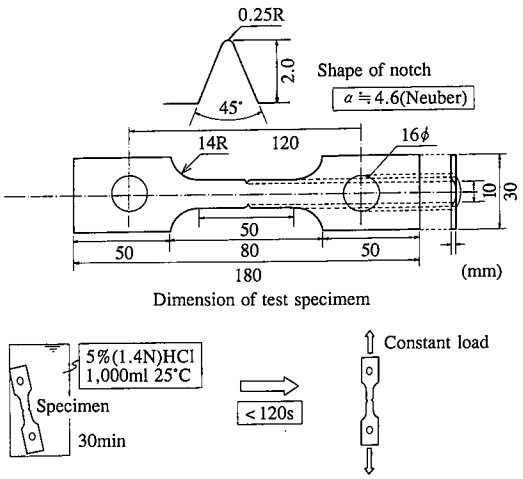

Fig. 14 Method for evaluating delayed fracture resistance

4.3 Absorbed energy

When the bending span that corresponds to the door size changes, flexural rigidity and intensities of flattening, plastic collapse and circumferential buckling change. As a result, the displacement-load curve in the three-point bend test greatly changes.[2] As shown in **Fig. 16**, however, the energy (elastic deformation energy plus plastic deformation energy) absorbed by

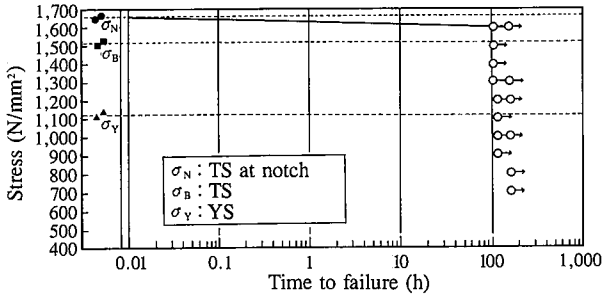

Fig. 15 Delayed fracture

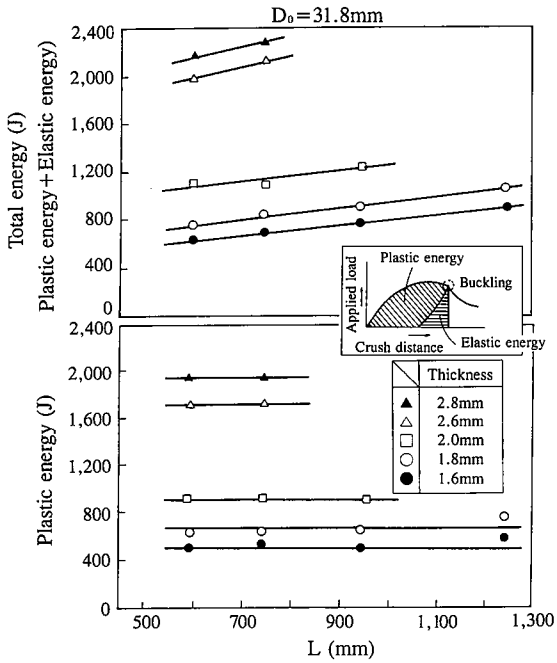

Fig. 16 Absorbed energy before onset of circumferential buckling

the tube through its bending deformation until its circumferential buckling depends on the wall thickness, and the absorbed energy due to the plastic deformation is little affected by the bending span. This is because the plastic deformation is concentrated right below the loading device, as shown in **Fig. 4**, for example.

When the door impact beam tube is considered as a member for preventing the door from intruding into the passenger compartment on a side collision, the energy absorbed by it until a given displacement (for example, 6 inches) is important. **Fig. 17** shows the absorbed energy before the 6-inch crush. The absorbed energy may be divided into two regions according to whether or not the absorbed energy is influenced by circumferential buckling[2]. For the 600-mm bending span that simulates a small door size, the absorbed energy can be increased by increasing the wall thickness in the region where the onset of circumferential buckling is delayed by the increased wall thickness. For the 1,250 mm bending span that simulates a large door size, a thin-walled tube does not circumferentially buckle, and the increase of absorbed energy with the increase of wall thickness works only to raise the maximum load. The boundary between the two regions in **Fig. 17** is the circumferential buckling condition at the 6-inch crush[2]. To obtain such a tube shape as to

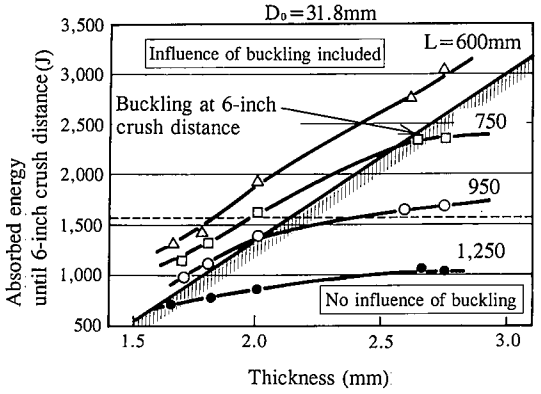

Fig. 17 Absorbed energy until 6-inch crush distance

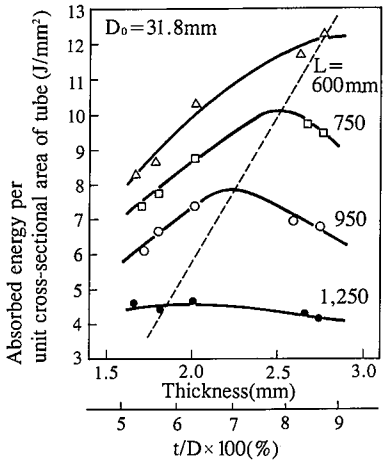

Fig. 18 Absorbed energy per unit cross-sectional area of tube

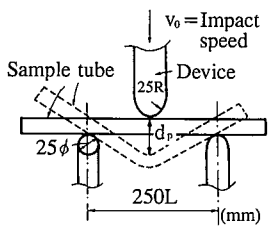

	Absorbed energy
Static	$E_S=\int_0^{\delta_P+\delta_E} P(\delta)d\delta$ δ_P : Plastic crush Distance δ_E : Elastic crush Distance
Impact	$E_I=m\cdot g\cdot h$ m: Loading device weight h: Drop weight height

Fig. 19 High-speed bending test method

increase the absorbed energy on bending, the absorbed energy shown in **Fig. 17** was divided by the cross-sectional area of the tube to obtain the absorbed energy on bending per cross-sectional area (or weight). The results are given in **Fig. 18**. From **Fig. 18**, it can be seen that there is the t/D ratio at which light weight and high absorbed energy can be achieved for each bending span or door size. For the bending span of 800 mm and tube outside diameter of 31.8 mm, for example, the absorbed energy per weight is maximum at the wall thickness of 2.4 mm.

The bending deformation behavior and absorbed energy of door impact beam tubes have been discussed above. The high-speed deformation that simulates an actual collision is briefly described here. A high-speed bending test method is schematically shown in **Fig. 19**. The absorbed energy on bending was

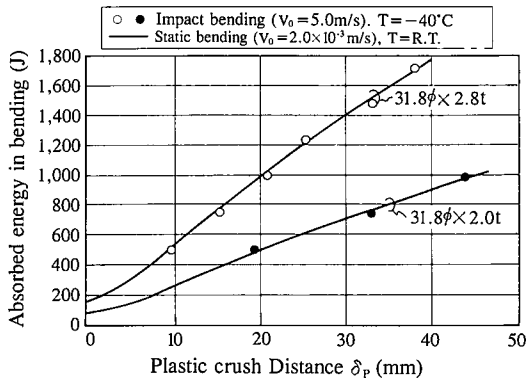

Fig. 20 Comparison of absorbed energy during static bending test and impact bending test (31.8 mm ϕ × 2.8 mm t, 2.0 mm t)

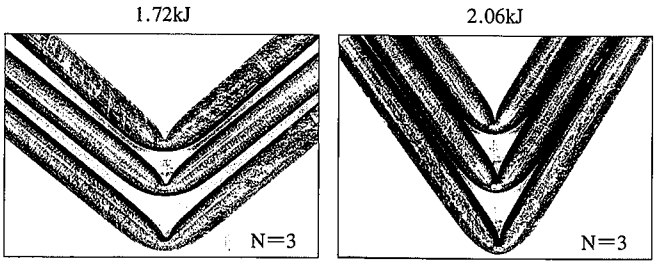

Photo 2 Appearance of sample tubes after impact bending at 233 K (25.4 mm ϕ × 2.3 mm t)

calculated from the area below the crush distance-applied load curve as shown in **Fig. 1** for low-speed bending and from the kinetic energy of the loading device for high-speed bending. **Fig. 20** compares the absorbed energy on high-speed deformation (at the loading device initial speed v_0 of 5.0 m/s) and that on low-speed deformation (at v_0 of 2.0×10^{-3} m/s). The values of absorbed energy on high-speed deformation as indicated by solid and open circles agree well with those of absorbed energy on bending deformation as indicated by solid lines.

Generally, the flow stress of body-centered cubic (bcc) metals depends on the strain rate ($\dot{\varepsilon}$), and the m value ($m = \partial \ln \sigma / \partial \ln \dot{\varepsilon}$ for pure iron is reported to range from 0.02 to 0.04[1]). When the new door impact beam tube steel was tension tested in the wide strain rate range of 10^{-3} to 10^{0} s^{-1}, its m value was small ($m < 0.001$) and was not dependent on the strain rate[2]. This suggests that the flow stress of the steel during high-speed deformation as in collision can be estimated from its static deformation behavior.

Photo 2 shows the appearance of tubes bent at high speed and 233 K. Each tube absorbed energy of about 2 kJ (average passenger car weight × 6 inches) and did not reveal brittle fracture or other defects at the test temperature.

5. Conclusions

Steel tubes for door impact beams were three-point bend tested to study their deformation behavior and clarify the deformation process. A new electric resistance welded (ERW) tube with high strength, ductility, and toughness as required for door impact beams was developed. This high-strength ERW tube was found to have a satisfactory energy absorbing capacity in the service environment of door impact beams.

References

1) Tanabe, H., Yamazaki, K.: CAMP-ISIJ. 4, 543 (1991)
2) Tanabe, H. et al.: Tubing for the Automobile Industry. Detroit, 1991, ITA, p. 95
3) Endo, J., Murota, T.: J. Jpn. Soc. Technol. Plast. 23 (258), 708 (1982)
4) Murota, T., Endo, J.: J. Jpn. Soc. Technol. Plast. 23 (255), 343 (1982)
5) Endo, J., Murota, T.: J. Jpn. Soc. Technol. Plast. 27 (301), 314 (1986)
6) Sudo, M., Hashimoto, S., Kanbe, A.: Tetsu-to-Hagané. 68, 1211 (1982)
7) Hashimoto, S., Mimura, K., Hosoda, T., Sudo, M.: Tetsu-to-Hagané. 72, 1736 (1986)
8) Pickering, F.B. et al.: JISI. (9), 66 (1960)
9) Hodge, J.M. et al.: Trans. Metall. Soc. AIME. 167, 627 (1946)
10) Ueno, M., Ito, K.: Tetsu-to-Hagané. 74, 910 (1988)
11) Sakui, S., Sakai, T.: Tetsu-to-Hagané. 58, 1438 (1972)